SEYBOLD Report
ISSN: 1533 - 9211
DOI: 10.5281/zenodo.6850778

MODELING AND EXPERIMENTAL VALIDATION OF EQUIVALENT CIRCUIT MODEL OF LITHIUM ION BATTERY FOR SUSTAINABLE TRANSPORTATION

Sagar B S
Assistant Professor, School of Electrical and Electronics Engineering, REVA University, Bengaluru, Karnataka 560064, India, sagar.bs14@gmail.com

Santoshkumar Hampannavar
Professor, School of Electrical and Electronics Engineering, REVA University, Bengaluru, Karnataka 560064, India, santoshkumar.sh@ieee.org

Bansilal Bairwa
Assistant Professor, School of Electrical and Electronics Engineering, REVA University, Bengaluru, Karnataka 560064, India, bansilalbairwa@gmail.com

Swapna M
Assistant Professor, Department of Electrical and Electronics Engineering, National Institute of Technology, Silchar, Assam 788010, India, swapna@ee.nits.ac.in

Abstract - Sustainable transportation requires employability of electric vehicles (EVs). The battery powered vehicles are to compete with internal combustion engines in terms of run time, reliability and maintainability. Battery management system (BMS) deployed in electric vehicles are powered with monitoring and controlling key aspects of battery. Battery modeling plays a key role in adding the BMS with necessary parameters which helps in having a controlled and required level of charging and discharging of batteries and predicting the behavior of battery at harsher conditions like in electric vehicles. Various battery models were reviewed. Equivalent circuit model (ECM) for lithium ion battery was proposed. Proposed model was experimentally tested at different temperatures subjecting to different drive cycles and was validated. The work provides effective solution in replicating the battery behavior in real time considering EV applications

Keywords - *Battery, modelling, equivalent circuit model, drive cycle, electric vehicle*

I. Introduction

Environmental pollution, global warming and depleting fossil fuels are the cause to look at alternative solutions to internal combustion engine (ICE) powered vehicles. The need for reduction is evident as the global temperature is surging up at an alarming rate. According to 2020 Production Gao report, world needs to reduce annual production of fossil fuels by 6% to limit the global increase in temperature to 1.5o C. Between 2020 to 2030, global gas, oil and coal production has to drop down by 3%, 4% and 11 % to be on lines with 1.5° C [1]-[2]. The world's most efficient ICE powered by diesel which is two stroke turbo charged low speed engine designed by Finnish manufacturer shown in figure 1, has 57% efficiency while for the gasoline engine has 40%. The overcome all these difficulties are by employing battery powered vehicles. Performance of the electric motor is superior in terms of torque and power density and also can maintain very good efficiency. Electric Motor named as Remy HVH410-075-DOM is shown in figure 2 has maximum efficiency of 95% [3]. Thus, employing battery as

SEYBOLD Report
ISSN: 1533 - 9211
DOI: 10.5281/zenodo.6850778

power source to the vehicles will be the key towards sustainable solution.

The battery powered vehicles which can also be termed as electric vehicles can be grouped into four major divisions namely: battery electric vehicle (BEV), plug-in hybrid electric vehicle (PHEV), extended range electric vehicle (EREV), hybrid electric vehicle (HEV) and fuel cell electric vehicle (FCEV). The divisions with example is shown in figure 3 [4]-[6].

It is to be noted that, battery is major source across the divisions. The battery converts its chemical energy into electric energy powering up the vehicle. This battery has to provide energy to drive the vehicle and also to recycle during braking period of the vehicle called as regenerative braking. Various battery chemistries can be employed in electric vehicles however each chemistry has its own advantages and limitations which are tabulated as below. From the comparative study, it is observed that lithium ion batteries are more suitable for powering up EVs. The performance tradeoff for a battery is shown in spider diagram in figure 4 as compared to ICE engines [7].

Fig. 1. Diesel Engine - Wärtsilä-Sulzer RTA96-C

Fig. 2. Electric motor - Remy HVH410-075-DOM

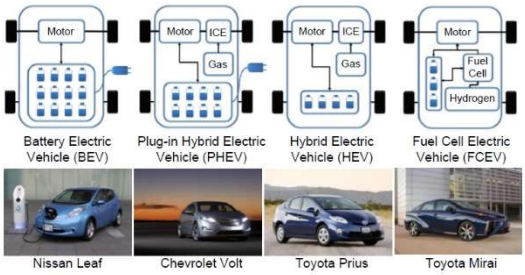

Fig. 3. Categories of electric vehicles

TABLE 1.
BATTERY SPECIFICATIONS

SEYBOLD Report
ISSN: 1533 - 9211
DOI: 10.5281/zenodo.6850778

Parameter	Units	Lead-acid type	Nickel Metal battery	Lithium ion battery
Battery Voltage	V	2	1.2	3.3. to 3.7
Energy density	Wh/kg	35 – 40	60 to 80	100 to 250
Specific energy	Wh/L	60 – 80	180 to 200	300 to 400
Life time of the battery	Number of cycles	300 to 500	500 to 1200	800 to 2000
Self- discharge rate	% per month	5 to 10	10 to 30	Less than 3%
Memory effect	-	No	Yes	No
Response to unfair usage	-	Very good	Good	Fair
Impact to environment	-	Highly toxic	Less toxic	Less toxic
Cost	-	Low	Medium	High

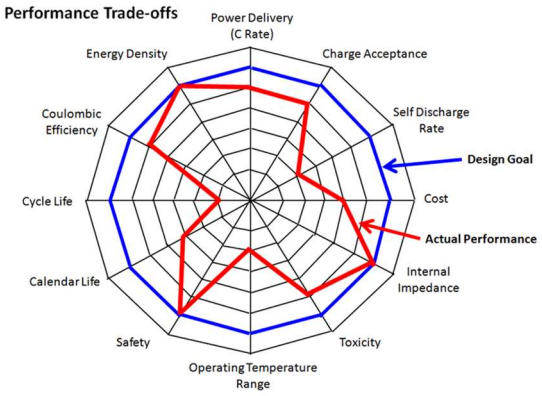

Fig. 4. Spider chart representing present performance of Li-ion batteries in comparison to 15-year life cycle and 5000 recharge cycles as per FreedomCAR reports (Chart courtesy Venkat Srinivasan and Vince Battaglia)

II. Literature Review and Proposed Work

Lithium ion batteries as employed to power up the electric vehicle, it is still an enigma as to its efficient employability. Even though the lithium based batteries are having high energy density, it has low or zero resistance to any voltage abuse. The operations like over charging, over discharging, variation in operating temperature would severely harm the batteries resulting in degradation in its performance, reduction in the life time and potential threat of explosion. Therefore, a managing system to monitor the battery pack is essential for battery powered vehicles. The major functions of battery management system (BMS) are voltage monitoring and protection, current monitoring and protection, charge and discharge monitoring, temperature monitoring, state of charge estimation and charge balancing. The diagrammatic representation of BMS is shown in figure 5.

SEYBOLD Report
ISSN: 1533 - 9211
DOI: 10.5281/zenodo.6850778

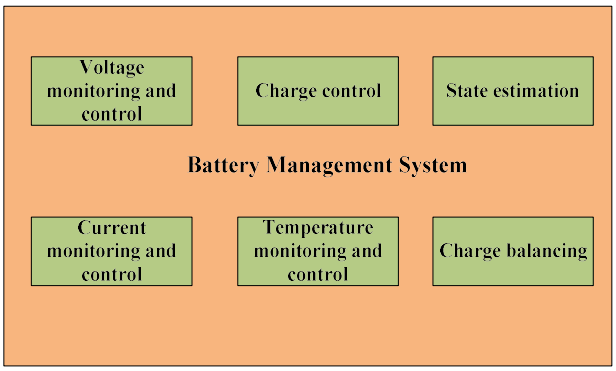

Fig. 5. Overview of battery management system (BMS)

The key aspect in battery management system is in estimating the state of charge of the battery and predicting the run time of the vehicle. Incorrect estimation results in decreasing the life time of battery as the SOC has direct impact on charge control thereby degrading the capacity of the battery. Driver's decision on run time and mileage is impacted. Incorrect estimation also has high impact on vehicle's maintainability which leads to heavy re-investment in replacing the abused and malfunctioning battery pack. Hence a reliable battery model is necessary to predict the behavior of the battery and estimating its parameters for employability and effective utilization of the battery pack of electric vehicles.

Various lithium ion battery models have been developed by researchers and numerous state estimation algorithms have been considered to estimate the parameters. However, these models come with different approximations and assumptions. Also the degree of complexity varies with different models thereby limiting the employability of these models on case specific. The models can be categorized into electro-chemical models, impedance spectroscopy models, empirical models, black box models and equivalent circuit models.

II.1. Electro-chemical models

These models employ the physical actions that occurs inside the battery to characterize its behavior. Partial differential equations are developed to represent battery behavior. These models are preferred for critical applications only as these are complex and require more computationally equipped processors to develop the models. They are also referred to as first principal models. These models are best fit to provide the state of charge and state of health of the battery however, on-board battery management systems seek reduced model to provide the results in less time and reduce computational stress. Another major factor in limited employment of these models is that the model requires multiple parameters such electrode dimensions, diffusion coefficients, viscosity to name a few. They are also termed as first-principal models and employ partial differential equations to describe the model. considering the lithium battery, mathematical model for positive electrode can be given as in equations 1 and 2. Equation 1 represents for solid phase positive electrode and equation 2 represents for represents for liquid phase positive electrode.

$$\frac{d}{dx}(D_{s,3}^{\ eff}\frac{d}{dx}\varphi_{s,3}^{\ eff}(x,t))=f_{s,3}(x,t) \qquad (1)$$

$$f_{s,3}(x,t)=\frac{d}{dx}k_{e,3}^{D,eff}\frac{d\ln C_{e,3}(x,t)}{dx} \qquad (2)$$

SEYBOLD Report
ISSN: 1533 - 9211
DOI: 10.5281/zenodo.6850778

Where the above two equations are subjected to specific boundary condition

$D_{s,3}^{eff}$ - diffusion coefficient

$\varphi_{s,3}^{eff}$ - potential in solid phase

K – conductivity of liquid solution

$f(x,t)$ - current density

Porous electrochemical model proposed by J S Newman is widely employed [8]. Based on the same, with few modifications other electro chemical models are employed in [9]-[11]. Doyle developed one dimensional isothermal electrochemical model for various battery types [12]. Inclusion of galvanostatic boundary condition in electrochemical model resulted better analysis while increasing the complexity of the model in [13].

II.2. Impedance spectroscopy model

Electrochemical impedance spectroscopy method is employed to obtain AC equivalent models in frequency domain which includes RLC networks to best fit impedance spectra. The model is shown in figure 6 along with measured impedance spectroscopy in figure 7. These impedance models work only for fixed SOC and temperature parameters which are highly unlikely to occur in real-time battery powered applications like electric vehicles [14].

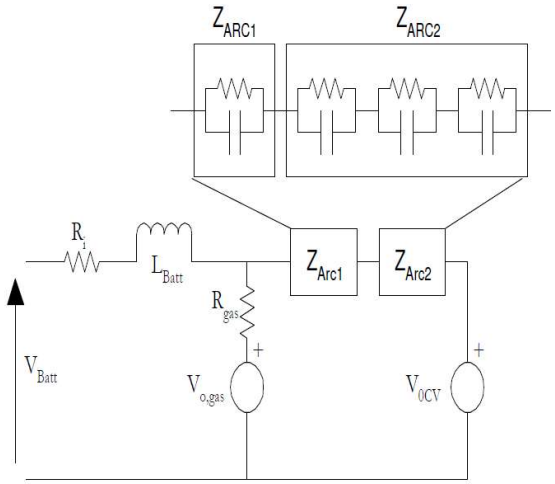

Fig. 6. Impedance spectroscopy circuit

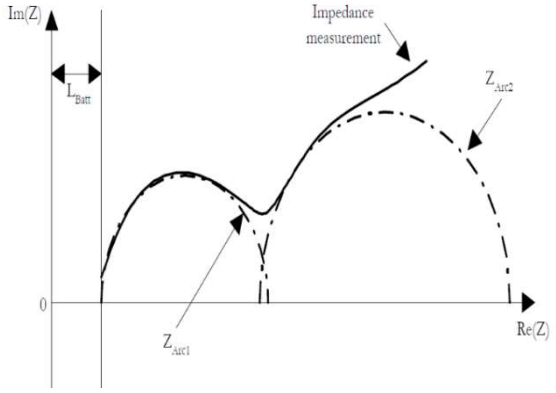

Fig. 7. Impedance measurement of the model

R_i - Battery internal resistance

SEYBOLD Report
ISSN: 1533 - 9211
DOI: 10.5281/zenodo.6850778

V_{oc} – open circuit voltage
L_{batt} – battery inductance
R_g and V_g – gassing reactions inside battery
Z_{Arc1} and Z_{Arc2} – complex inductance of the model

II.3. Emperical model

Peukert's relation is the prime model described under this category of battery model. The relation between the charge capacity Q and the current I can be given by the equation 1. In the equation t_{cutoff} specifies the time required to reach rated cut off voltage. For constant current discharge mode, Peukert's equation is represented in equation 2 where I represent constant discharge current and Peukert exponent, n, depends on battery manufacture and □□and n are curve fitting constants.

The exponent values vary with time which makes further estimation of SOC and other battery parameters difficult. Using equations 3 and 4, I is obtained as represented in equation 5.

$$Q = I\, t_{cutoff} \quad (3)$$

$$I^n\, t_{cutof}\, f = \lambda \quad (4)$$

$$I^n \frac{Q}{I} = \lambda \quad (5)$$

Practical implementation of Peukert's equation using Peukert's capacity Cp is given in equation 6 where I represent battery current and n is the Peukert exponent for the discharge time T. Variation of the Peukert capacity according to the discharge current is the limitation to be considered.

$$C_p = I^n\, T \quad (6)$$

II.4. Black box models

These are the models developed for the system where internal chemistries or components are unknown. These models take into account only the external activity of the system. The models employ linear and non-linear functions to describe the behavior of batteries. Support vector machine (SVM) and stochastic fuzzy neural networks based models are developed in [15]-[16].

III. **Equivalent Circuit Model**

The equivalent circuit models are developed to represent the behavior of the battery using basic electrical components like resistors and capacitors and a simple voltage source.
Min Chen developed I-V performance prediction model [17]. Series equivalent circuit models were proposed by Plett [18], in which hysteresis is employed with dual Kalman filtering method. However, this method does not account for the stability analysis for the system. Joint extended Kalman filter were employed [19] which incorporated capacitor in equivalent circuit model as to represent battery capacity. Similar problem of stability encountered by these models also. Simultaneous action of modeling and parameter estimation from the model developed in [20] incorporating incremental capacity analysis (ICA) support vector regression algorithm (SVR) required high sampling rate and high resolution data processors which are difficult to

SEYBOLD Report
ISSN: 1533 - 9211
DOI: 10.5281/zenodo.6850778
realize in real time.
The artificial neural network based models has the problem of acquiring large scale training data from experimental tests and do not include aging mechanism of the battery [21]-[22]. Models considering the effect of temperature at low and high levels are developed in [23]-[24]. In total, battery modeling considering the battery parameter estimation, ageing and temperature impact on battery are not well accounted [25]-[28]. Some models are theoretically described and lack experimental justification.
The basic Thevenin model employs resistors representing internal resistance during cases of charging and discharging process aided by blocking diodes in either cases shown in figure 7. A voltage source with a capacitor emulates the nonlinear open circuit voltage is represented in figure 8. Series resistance can be included in the circuit as shown in figure 9 to represent the losses occurred when batteries are subjected to over-charging and over discharging process. A simplified approach to represent the battery behavior is shown in figure 10 where series resistor represents internal resistance of the battery and a bulk capacitor represents the non-linear open circuit voltage as well as charge depletion status of the battery. Equation (7) represents terminal voltage.

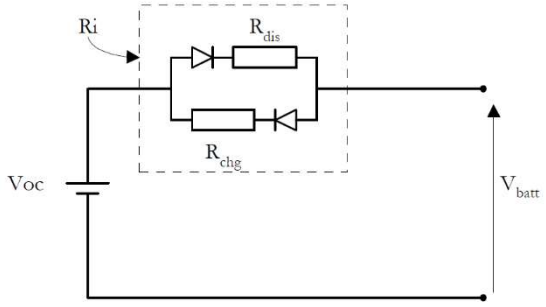

Fig. 7. Basic Thevenin circuit

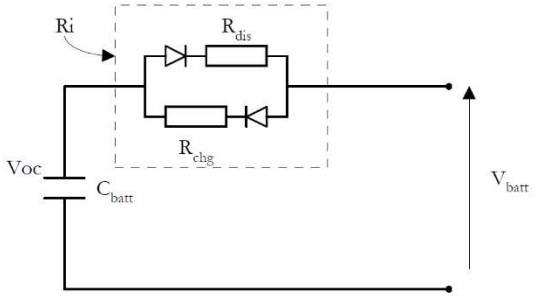

Fig. 8. Modified Thevenin circuit with capacitor

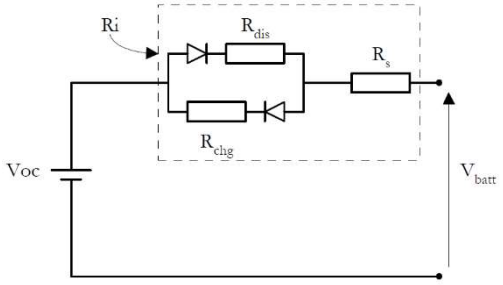

Fig. 9. Modified Thevenin circuit with series resistance

SEYBOLD Report
ISSN: 1533 - 9211
DOI: 10.5281/zenodo.6850778

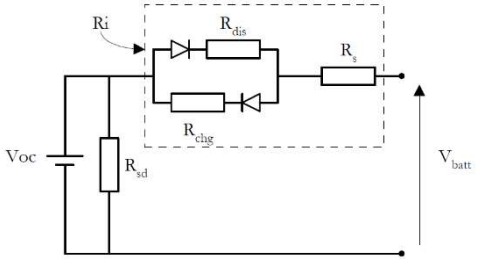

Fig. 10. Modified Thevenin circuit with internal resistance

$$V_L(i) = OCV[SOC(i)] - I(i)R_0 \qquad (7)$$

Where i represents the discreet step and $V_L(i)$ represents terminal voltage of the battery OCV[SOC(i)] represents open circuit voltage taken as function of SOC, I(i) represents input current which is positive value for charging state and negative for discharge state and R0 represents internal resistance of the battery. For the above model, the zero state hysteresis model is described in equation (8) and (9).

$$V_L(i) = OCV(SOC(i)) - I(i)R_0 - g(i)H \qquad (8)$$

$$g(i) = \begin{Bmatrix} \mathbf{1} & I(i) > \mu \\ -\mathbf{1} & I(i) < \mu \\ g(i-\mathbf{1}) & \end{Bmatrix} \qquad (9)$$

Where H is hysteresis effect and μ represents positive dead band constant.

III.1. *Proposed RC models*

A more profound RC models are developed for batteries are shown in figures 11 to 14. Equations representing the models from equation 10 to equation 44 are represented along with the corresponding models.

III.1.1 1 RC model

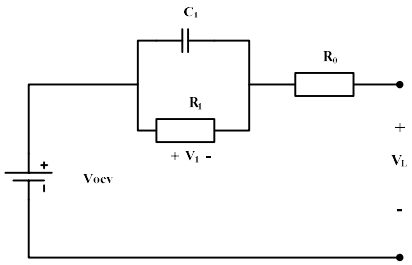

Fig. 11. 1 RC equivalent circuit model

$$V_L(n) = OCV(SOC(n)) - I(n)R_0 - U_1(n) \qquad (10)$$

$$U_1(n+1) = e^{\left(-\frac{\Delta t}{\tau_1}\right)} U_1 n + R_1\left(1 - e^{\left(-\frac{\Delta t}{\tau_1}\right)}\right) I(n) \qquad (11)$$

$$\tau_1 = R_1 C_1 \qquad (12)$$

III.1.2 2 RC Model

SEYBOLD Report
ISSN: 1533 - 9211
DOI: 10.5281/zenodo.6850778

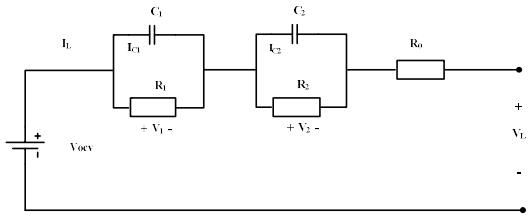

Fig. 12. 2 RC equivalent circuit model

$$V_L(n)=OCV(SOC(n))-I(n)R_0-U_1(n)-U_2(n) \quad (13)$$

$$U_1(n+1)=e^{(-\frac{\Delta t}{\tau_1})}U_1 n+R_1(1-e^{(-\frac{\Delta t}{\tau_1})})I(n) \quad (14)$$

$$U_2(n+1)=e^{(-\frac{\Delta t}{\tau_2})}U_2 n+R_2(1-e^{(-\frac{\Delta t}{\tau_2})})I(n) \quad (15)$$

$$\tau_1=R_1C_1 \quad (16)$$

$$\tau_2=R_2C_2 \quad (17)$$

III.1.3 3 RC Model

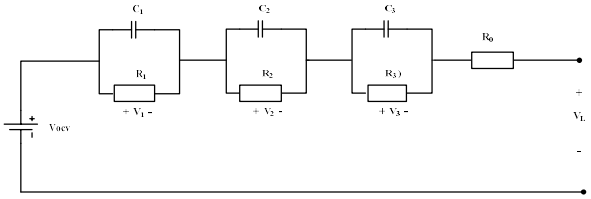

Fig. 13. 3 RC equivalent circuit model

$$V_L(n)=OCV(SOC(n))-I(n)R_0-U_1(n)-U_2(n)-U_3(n) \quad (18)$$

$$U_1(n+1)=e^{(-\frac{\Delta t}{\tau_1})}U_1 n+R_1(1-e^{(-\frac{\Delta t}{\tau_1})})I(n) \quad (19)$$

$$U_2(n+1)=e^{(-\frac{\Delta t}{\tau_2})}U_2 n+R_2(1-e^{(-\frac{\Delta t}{\tau_2})})I(n) \quad (20)$$

$$U_3(n+1)=e^{(-\frac{\Delta t}{\tau_3})}U_3 n+R_3(1-e^{(-\frac{\Delta t}{\tau_3})})I(n) \quad (21)$$

$$\tau_1=R_1C_1 \quad (22)$$

$$\tau_2=R_2C_2 \quad (23)$$

$$\tau_3=R_3C_3 \quad (24)$$

III.1.4 4 RC Model

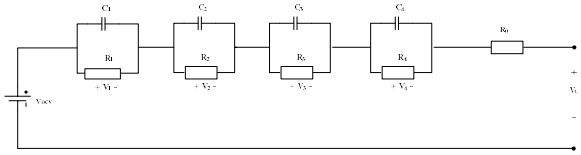

Fig. 14. 4 RC equivalent circuit model

$$V_L(n)=OCV(SOC(n))-I(n)R_0-U_1(n)-U_2(n)-U_3(n)-U_4(n) \quad (25)$$

$$U_1(n+1)=e^{(-\frac{\Delta t}{\tau_1})}U_1 n+R_1(1-e^{(-\frac{\Delta t}{\tau_1})})I(n) \quad (26)$$

$$U_2(n+1)=e^{(-\frac{\Delta t}{\tau_2})}U_2 n+R_2(1-e^{(-\frac{\Delta t}{\tau_2})})I(n) \quad (27)$$

$$U_3(n+1)=e^{(-\frac{\Delta t}{\tau_3})}U_3 n+R_3(1-e^{(-\frac{\Delta t}{\tau_3})})I(n) \quad (28)$$

$$U_4(n+1)=e^{(-\frac{\Delta t}{\tau_4})}U_4 n+R_4(1-e^{(-\frac{\Delta t}{\tau_4})})I(n) \quad (29)$$

$$\tau_1=R_1C_1 \quad (30)$$

SEYBOLD Report
ISSN: 1533 - 9211
DOI: 10.5281/zenodo.6850778

$$\tau_2 = R_2C_2 \quad (31)$$

$$\tau_3 = R_3C_3 \quad (32)$$

$$\tau_4 = R_4C_4 \quad (33)$$

III.1.5 5 RC Model

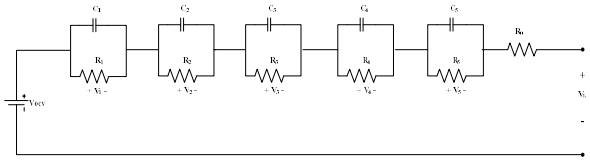

Fig.15. 5 RC equivalent circuit model

$$V_L(n) = OCV(SOC(n)) - I(n)R_0 - U_1(n) - U_2(n) - U_3(n) - U_4(n) - U_5(n) \quad (34)$$

$$U_1(n+1) = e^{(-\frac{\Delta t}{\tau_1})} U_1 n + R_1 (1 - e^{(-\frac{\Delta t}{\tau_1})}) I(n) \quad (35)$$

$$U_2(n+1) = e^{(-\frac{\Delta t}{\tau_2})} U_2 n + R_2 (1 - e^{(-\frac{\Delta t}{\tau_2})}) I(n) \quad (36)$$

$$U_3(n+1) = e^{(-\frac{\Delta t}{\tau_3})} U_3 n + R_3 (1 - e^{(-\frac{\Delta t}{\tau_3})}) I(n) \quad (37)$$

$$U_4(n+1) = e^{(-\frac{\Delta t}{\tau_4})} U_4 n + R_4 (1 - e^{(-\frac{\Delta t}{\tau_4})}) I(n) \quad (38)$$

$$U_5(n+1) = e^{(-\frac{\Delta t}{\tau_5})} U_5 n + R_5 (1 - e^{(-\frac{\Delta t}{\tau_5})}) I(n) \quad (39)$$

$$\tau_1 = R_1C_1 \quad (40)$$

$$\tau_2 = R_2C_2 \quad (41)$$

$$\tau_3 = R_3C_3 \quad (42)$$

$$\tau_4 = R_4C_4 \quad (43)$$

$$\tau_5 = R_5C_5 \quad (44)$$

III.2. Drive Cycles

The United States Advanced Battery Consortium (USABC) has developed and standardized the battery test procedures by all testing organizations. According to USABC, two modes of discharge test have been defined for batteries namely, constant power discharge test and variable power discharge test. According to constant power discharge test, battery is made to discharge at set power levels. Minimum of 3 power levels are identified, nominally required to discharge 75% of rated energy from the battery in one hour. Further, the reduced power levels are defined at 2/3 and 1/3 of this maximum power level, respectively. Electric vehicle driving behavior is simulated in variable power discharge testing method which includes the action of regenerating braking. Federal Urban Driving Schedule (FUDS) procedure, which is a complex 1372 second time-velocity profile based on actual driving data, is employed. Dynamic Stress Test (DST) is a simplified variable power discharge cycle with the same average characteristics as FUDS. DST uses 360 second sequence of power steps with only 7 discrete power levels. Beijing Dynamic Stress Test (BJDST) is also utilized to test the battery.

III.3. RMSE Analysis

The developed battery models are experimentally validated. The model data and tested data are subjected to root mean square error (RMSE) analysis given in the equation 45 to find out the model's correctness. RMSE is the standard deviation of predicted values with the actuals. Predicted values represents measure of how far from the regression line the data points are. It

SEYBOLD Report
ISSN: 1533 - 9211
DOI: 10.5281/zenodo.6850778

provides the information on how the data points are around the best fit.

$$\text{RMS error} = \sqrt{\frac{1}{n}\sum_{k=1}^{n}(x_k - y_k)^2} \qquad (45)$$

IV. Results and Discussion

Voltage response of developed RC models for DST and BJDST drive cycles at two different temperatures namely 25o C and 45o C are carried out. The results are shown in figures from figure 16 to figure 35. Analysis of developed RC models with respect to RMSE errors for DST and BJDST drive cycles carried out at 250 Celsius and 450 Celsius are tabulated as below. With this analysis, it can be declared that 3 RC model best fits the representation of battery behavior. This also signifies that if 3 RC model is employed for parameter estimation then it exhibits minimum error.

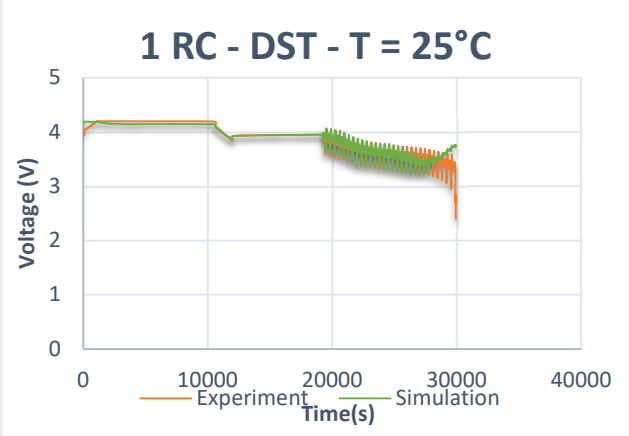

Fig. 16. 1RC circuit for DST at 25°C

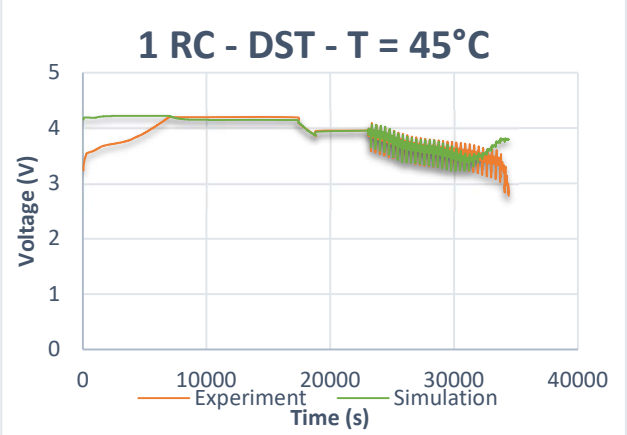

Fig. 17. 1RC circuit for DST at 45°C

SEYBOLD Report
ISSN: 1533 - 9211
DOI: 10.5281/zenodo.6850778

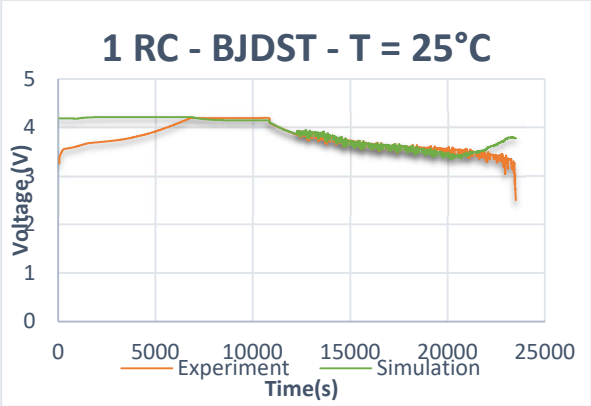

Fig. 18. 1RC circuit for BJDST at 25ºC

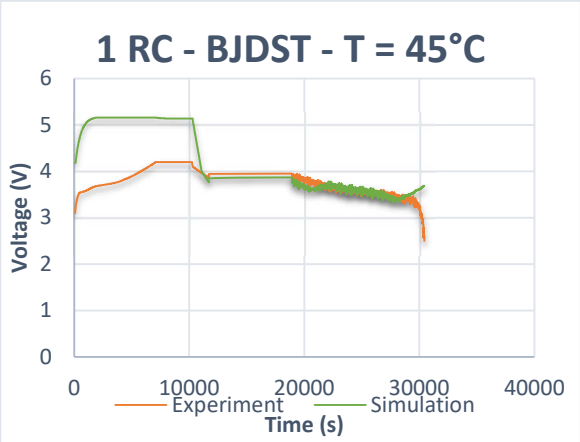

Fig. 19. 1RC circuit for BJDST at 45ºC

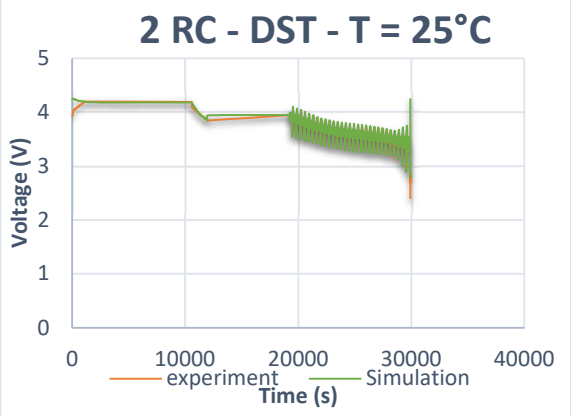

Fig. 20. 2RC circuit for DST at 25ºC

SEYBOLD Report
ISSN: 1533 - 9211
DOI: 10.5281/zenodo.6850778

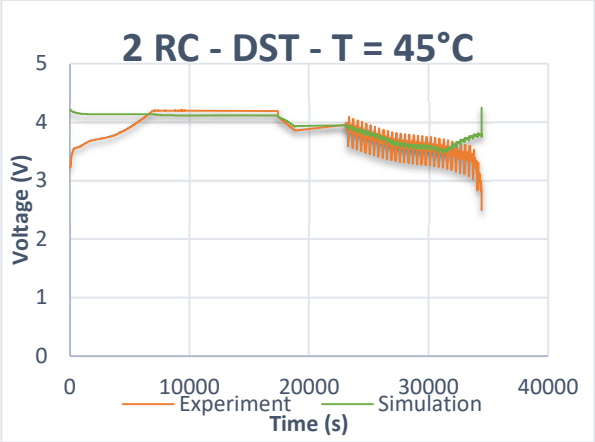

Fig. 21. 2RC circuit for DST at 45°C

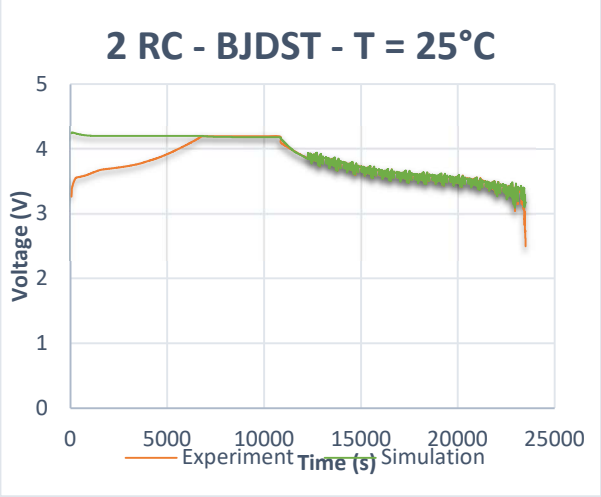

Fig. 22. 2RC circuit for BJDST at 25°C

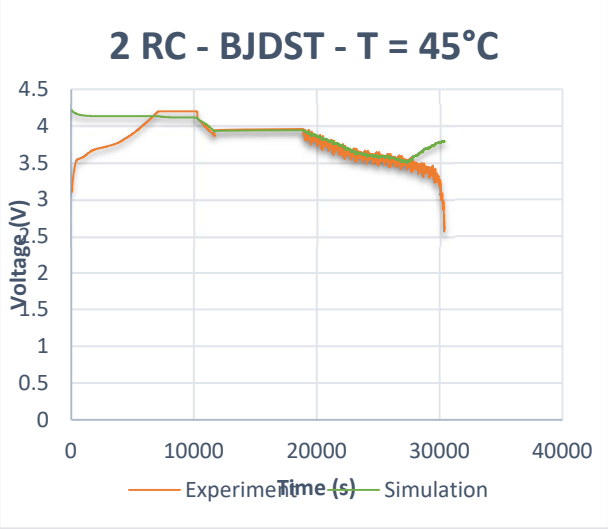

Fig. 23. 2RC circuit for BJDST at 45°C

SEYBOLD Report
ISSN: 1533 - 9211
DOI: 10.5281/zenodo.6850778

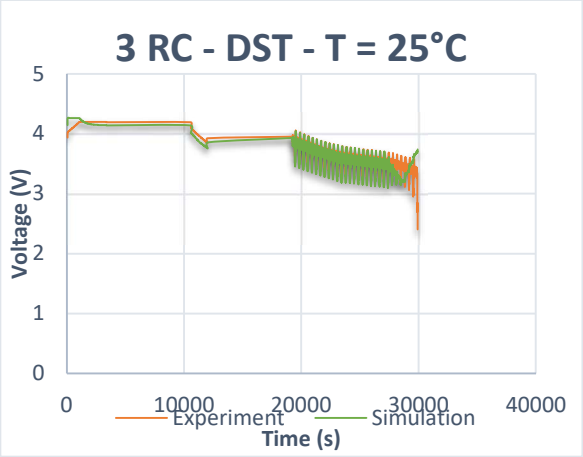

Fig. 24. 3RC circuit for DST at 25°C

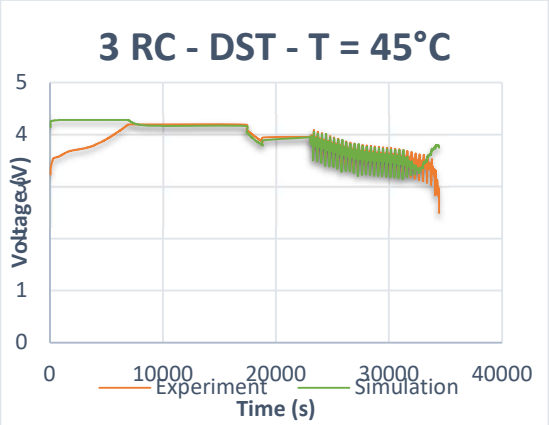

Fig. 25. 3RC circuit for DST at 45°C

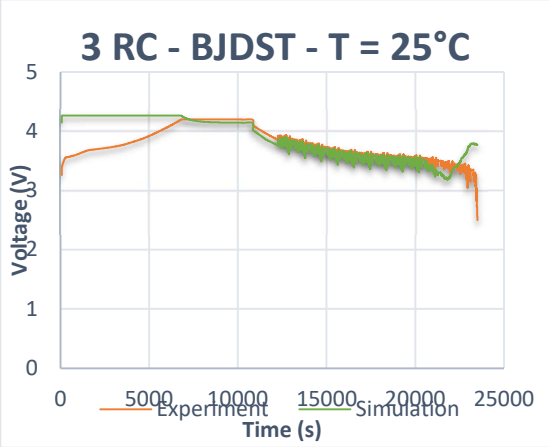

Fig. 26. 3RC circuit for BJDST at 25°C

SEYBOLD Report
ISSN: 1533 - 9211
DOI: 10.5281/zenodo.6850778

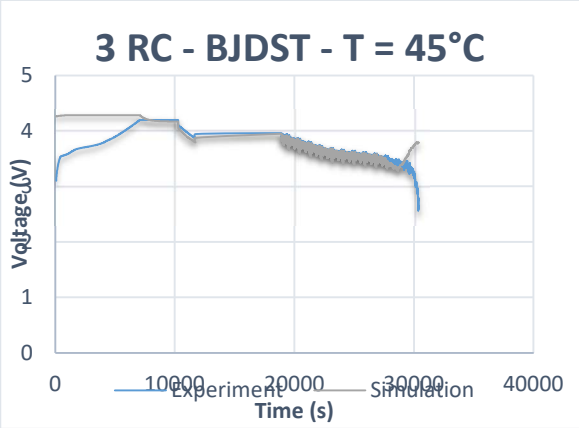

Fig. 27. 3RC circuit for BJDST at 45ºC

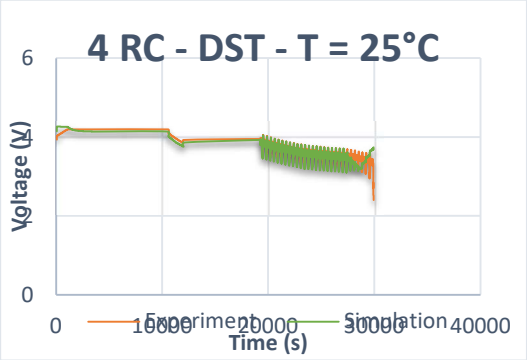

Fig. 28. 4RC circuit for DST at 25ºC

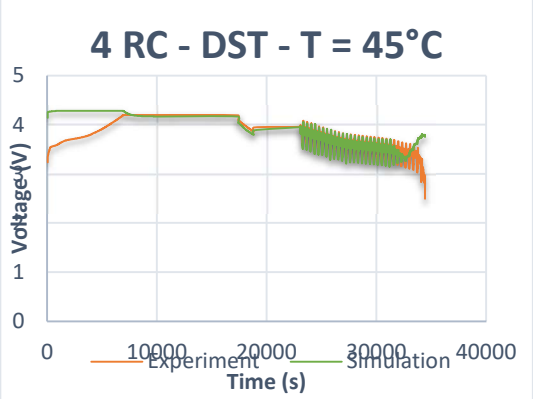

Fig. 29. 4RC circuit for DST at 45ºC

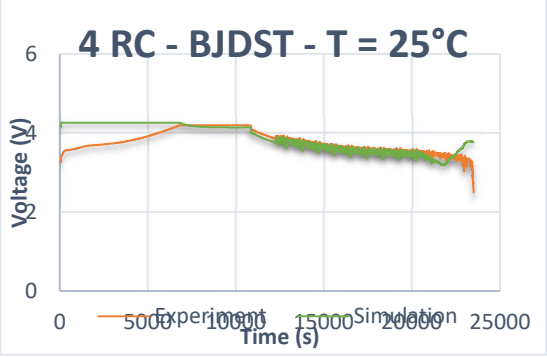

SEYBOLD Report
ISSN: 1533 - 9211
DOI: 10.5281/zenodo.6850778

Fig. 30. 4RC circuit for BJDST at 25ºC

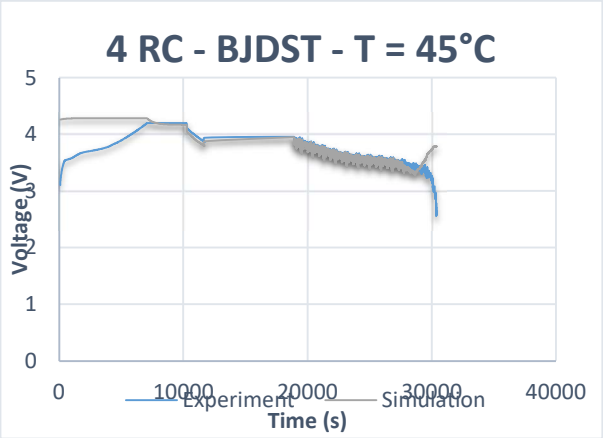

Fig. 31. 4RC circuit for BJDST at 45ºC

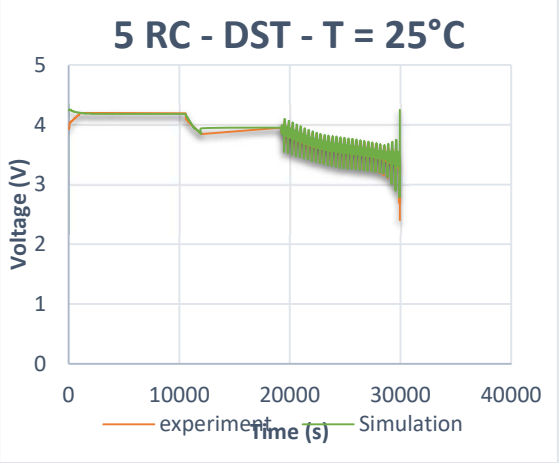

Fig. 32. 5RC circuit for DST at 25ºC

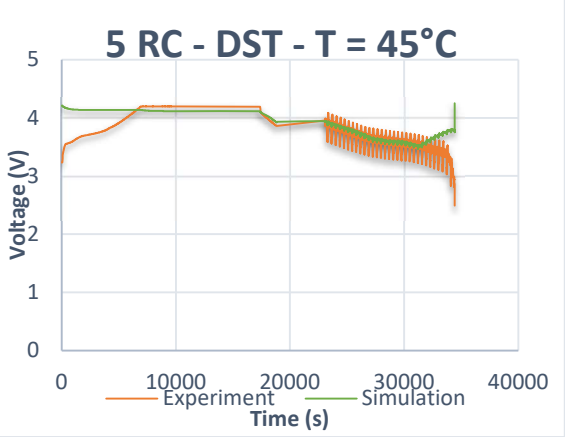

Fig. 33. 5RC circuit for DST at 45ºC

SEYBOLD Report
ISSN: 1533 - 9211
DOI: 10.5281/zenodo.6850778

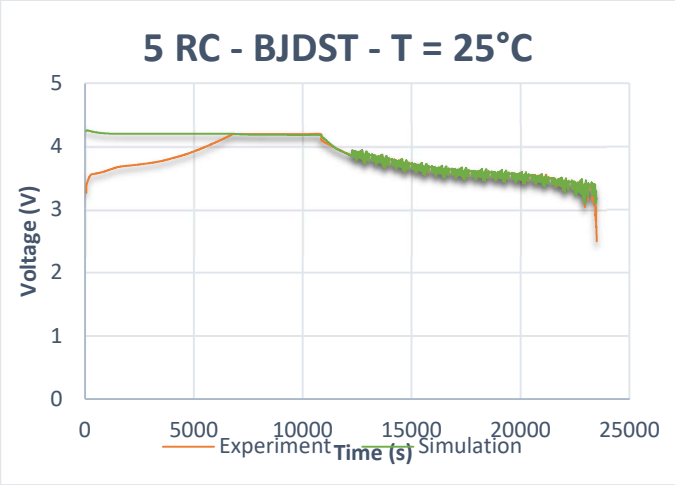

Fig. 34. 5RC circuit for BJDST at 25ºC

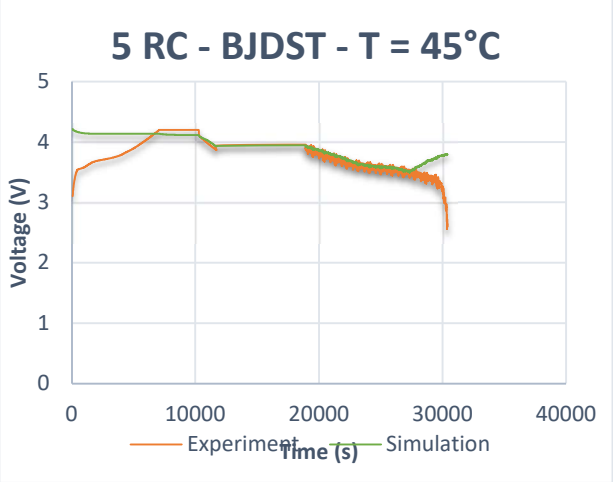

Fig. 35. 5RC circuit for BJDST at 45ºC

TABLE 2.
RMSE FOR 1 RC AND 2 RC MODEL

Model ➔ Drive cycle ➔ Temperature ➔	1 RC		2 RC	
	25 °C	45 °C	25 °C	45 °C
DST	0.1232	0.2097	0.0519	0.217
BJDST	0.1849	0.375	0.1066	0.222

SEYBOLD Report
ISSN: 1533 - 9211
DOI: 10.5281/zenodo.6850778

TABLE 3.
RMSE FOR 3 RC MODEL

Model ➔ Drive cycle ➔ Temperature ➔	3 RC	
	25 °C	45 °C
DST	0.02733	0.1111
BJDST	0.03962	0.09284

TABLE 4.
RMSE FOR 4 RC AND 5 RC MODEL

Model ➔ Drive cycle ➔ Temperature ➔	4 RC		5 RC	
	25 °C	45 °C	25 °C	45 °C
DST	0.1204	0.1992	0.7431	0.2377
BJDST	0.1894	0.2085	0.7648	0.2428

V. Conclusion

Various battery modelling techniques were discussed and presented. Equivalent circuit model (ECM) consisting of RC network was presented. 1 RC to 5 RC ECM of battery were developed and simulated. Battery models were tested at 25o C and 45o C subjected to DST and BJDST driving cycles which best replicates the electric vehicle drive pattern. The results were verified and validated with experimental set up and it was found that the 3 RC network model best suits battery behavior for electric vehicle application.

Acknowledgment

The authors are thankful to Center for Advanced Life Cycle Engineering, University of Maryland, for providing the experimental test data. Also, authors are grateful to the testing facilities at Center for Energy and Environment, Malaviya National Institute of Technology, Jaipur (MNIT, Jaipur), India.

References

[1] C. Mi, M. A. Masrur, and D. W. Gao, Hybrid Electric Vehicles: *Principles and Applications with Practical Perspectives, John Wiley & Sons, 2011*
[2] https://www.unep.org/news-and-stories/press-release/worlds-governments-must-wind-down-fossil-fuel-production-6-year#:~:text=Between%202020%20and%202030%2C%20global,and%20gas%20production%20in%202020
[3] Wärtsilä Corporation, Retrieved from http://www.wartsila.com/.
[4] General Motors Company, Retrieved from http://www.gm.com

[5] Linden, T.B. Reddy, eds. Handbook of Batteries,3rd Edition, New York: The McGraw-Hill Companies, Inc.; 2002
[6] United States Advanced Battery Consortium. Goals for Advanced Batteries for EVs.
[7] https://www.bestmag.co.uk/breakthroughs-dont-always-make-better-batteries/
[8] J. S. Newman. Electrochemical Systems, Second edition, Englewood Cliffs: Prentice-Hall, 1991
[9] T. Fuller, M. Doyle, J. Newman, Simulation and optimization of the dual lithium ion insertion cell, *Journal of the Electrochemical Society, vol. 141, pp.1–10*
[10] M. Doyle, T. Fuller, J. Newman, Importance of the lithium ion transference number in lithium/polymer cells, *Electrochimica Acta vol. 39, pp.2073- 2081*
[11] T. Fuller, M. Doyle, J. Newman, Relaxation phenomena in lithium-ion-insertion cells, *Journal of the Electrochemical Society, vol. 141, pp.982–990*
[12] M. Doyle, Y. Fuentes, Computer simulations of a lithium-ion polymer battery and implications for higher capacity next-generation battery designs, *Journal of the Electrochemical Society, vol. 150, pp.706–7131*
[13] V. R. Subramanian, V. Boovaragavan, V. Ramadesigan, M. Arabandi, Mathematical model reformulation for lithium-Ion battery simulations: Galvanostatic Boundary Conditions, *Journal of the Electrochemical Society, vol. 156, pp.260–2711*
[14] E. Surewaard, M. Tiller, D. Lizen, and D. Linzen, A comparison of Different Methods for Battery and Supercapacitor Modeling, *presented at SAE Future Transportation Technology Conference- SAE Technical Paper Series 2003-01-2290, 2003*
[15] Buller, E. Karden, D. Kok, and R. W. D. Doncker, Modeling the Dynamic Behaviour of Supercapacitors Using Impedance Spectroscopy, *IEEE Transactions on Industrial Applications, vol. 38, pp. 1622- 1626, 2002*
[16] C.Weng, Y.Cui, J.Sun, H.Peng. On-board state of health monitoring of lithium-ion batteries using incremental capacity analysis with support vector regression, *Journal of Power Sources, vol. 235, pp.36–44*
[17] A.A. Hussein, Capacity fade estimation in electric vehicles Li-ion batteries using artificial neural networks, *Energy Conversion Congress and Exposition (ECCE), 2013 IEEE, pp. 677 –681*
[18] M. Chen,G. A. Rincon-Mora, Accurate electrical battery model capable of predicting runtime and I-V performance, *IEEE Transactions on Energy Conversion, vol. 21, pp. 504–511*
[19] A.A. Hussein, Capacity fade estimation in electric vehicles Li-ion batteries using artificial neural networks, *Energy Conversion Congress and Exposition (ECCE), 2013 IEEE, pp. 677 –681.*
[20] C.Weng, Y.Cui, J.Sun, H.Peng. On-board state of health monitoring of lithium-ion batteries using incremental capacity analysis with support vector regression, *Journal of Power Sources, vol. 235, pp.36–44*
[21] A.A. Hussein, Capacity fade estimation in electric vehicles Li-ion batteries using artificial neural networks, *Energy Conversion Congress and Exposition (ECCE), 2013 IEEE, pp. 677 –681*
[22] W. He, N. Williard, M. Osterman, M. Pecht, Prognostics of lithium-ion batteries based on Dempster–Shafer theory and the Bayesian Monte Carlo method, *Journal of Power Sources, vol. 196, pp.10314–10321*
[23] J.Yi, U.S.Kim, C.B.Shin, T.Han, S.Park, Modeling the temperature dependence of the discharge behavior of a lithium-ion battery in low environmental temperature, *Journal of Power Sources, vol. 244, pp.143–148*

DOI: 10.5281/zenodo.6850778

[24] S.S. Zhang, K. Xu, T.R. Jow, The low temperature performance of Li-ion batteries, *Journal of Power Sources, vol. 115, pp.137–140*

[25] Hampannavar, Santoshkumar, Chavhan, Suresh, Mansani, Swapna and Yaragatti, Udaykumar R.. Electric Vehicle Traffic Pattern Analysis and Prediction in Aggregation Regions/Parking Lot Zones to Support V2G Operation in Smart Grid: A Cyber-Physical System Entity, *International Journal of Emerging Electric Power Systems, vol. 21, no. 1, 2020, pp. 20190176. https://doi.org/10.1515/ijeeps-2019-0176*

[26] Santosh Kumar, R.Y. Udaykumar,Stochastic Model of Electric Vehicle Parking Lot Occupancy in Vehicle-to-grid (V2G), *Energy Procedia,Volume 90,2016,Pages 655-659,ISSN 1876-6102,https://doi.org/10.1016/j.egypro.2016.11.234.*

[27] Hampannavar, Santoshkumar, Chavhan, Suresh, Yaragatti, Udaykumar and Naik, Anant. Gridable Electric Vehicle (GEV) Aggregation in Distribution Network to Support Grid Requirements: A Communication Approach, *International Journal of Emerging Electric Power Systems, vol. 18, no. 3, 2017, pp. 20160239. https://doi.org/10.1515/ijeeps-2016-0239*

[28] Santoshkumar and R. Y. Udaykumar, Performance investigation of mobile WiMAX protocol for aggregator and electrical vehicle communication in Vehicle-to-Grid(V2G), *2014 IEEE 27th Canadian Conference on Electrical and Computer Engineering (CCECE), 2014, pp. 1-6, doi: 10.1109/CCECE.2014.6901031*